

The role of spin-flipping terms in hadronic transitions of $\Upsilon(4S)$

Jorge Segovia,^{*} David R. Entem,[†] and Francisco Fernández[‡]

*Grupo de Física Nuclear and Instituto Universitario de Física Fundamental y Matemáticas (IUFFyM)
Universidad de Salamanca, E-37008 Salamanca, Spain*

(Dated: November 6, 2018)

Recent experimental data on the $\Upsilon(4S) \rightarrow \Upsilon(1S)\eta$ and $\Upsilon(4S) \rightarrow h_b(1P)\eta$ processes seem to contradict the naive expectation that hadronic transitions with spin-flipping terms should be suppressed with respect those without spin-flip. We analyze these transitions using the QCD Multipole Expansion (QCDME) approach and within a constituent quark model framework that has been applied successfully to the heavy-quark sectors during the last years. The QCDME formalism requires the computation of hybrid intermediate states which has been performed in a natural, parameter-free extension of our constituent quark model based on the Quark Confining String (QCS) scheme. We show that i) the M1-M1 contribution in the decay rate of the $\Upsilon(4S) \rightarrow \Upsilon(1S)\eta$ is important and its suppression until now is not justified; ii) the role played by the $L = 0$ hybrid states, which enter in the calculation of the M1-M1 contribution, explains the observed enhancement in the $\Upsilon(4S) \rightarrow \Upsilon(1S)\eta$ decay width; and iii) the anomalously large decay rate of the $\Upsilon(4S) \rightarrow h_b(1P)\eta$ transition has the same physical origin.

PACS numbers: 12.38.-t, 12.39.Pn, 14.40.Pq, 14.40.Rt, 13.25.Gv

Keywords: Quantum Chromodynamics, potential models, heavy quarkonia, exotic mesons, hadronic decays of Quarkonia

I. INTRODUCTION

The general way of referring to an hadronic transition is [1]

$$\Phi_I \rightarrow \Phi_F + h, \quad (1)$$

where Φ_I and Φ_F stand, respectively, for the initial and final states of heavy quarkonium. The emitted light hadron(s), h , are kinematically dominated by single particle ($\pi^0, \eta, \omega, \dots$) or two particle ($2\pi, 2K, \dots$) states.

Hadronic transitions are important decay modes for low-lying heavy quarkonium states. For instance, the first observed hadronic transition $\psi(2S) \rightarrow J/\psi\pi\pi$ [2] has a branching fraction reported by the Particle Data Group (PDG) of $(52.58 \pm 0.43)\%$ [3]. Moreover, during the last years, hadronic transitions between heavy quarkonia have led to a remarkable series of discoveries helping either to establish new conventional heavy quarkonium states, like the $h_b(1P)$ and $h_b(2P)$ observed in the two-pion decay of the $\Upsilon(5S)$ [4] state, or to extract relevant information of the so-called ‘‘XYZ’’ states, like in the cases of $X(3872)$ [5–7] and $X(4260)$ [8].

The BaBar Collaboration has presented a systematic study of hadronic transitions between $\Upsilon(mS)$ ($m = 4, 3, 2$) and $\Upsilon(nS)$ ($n = 2, 1$) states, reporting the first observation of the $\Upsilon(4S) \rightarrow \Upsilon(1S)\eta$ [9]. The measured branching fraction for this decay is

$$\mathcal{B}(\Upsilon(4S) \rightarrow \Upsilon(1S)\eta) = (1.96 \pm 0.06 \pm 0.09) \times 10^{-4}, \quad (2)$$

which is puzzling larger than the branching fraction for $\Upsilon(4S) \rightarrow \Upsilon(1S)\pi^+\pi^-$, $(0.800 \pm 0.064 \pm 0.027) \times 10^{-4}$, with a ratio between them of

$$R_\eta[\Upsilon(4S)] = \frac{\Gamma(\Upsilon(4S) \rightarrow \Upsilon(1S)\eta)}{\Gamma(\Upsilon(4S) \rightarrow \Upsilon(1S)\pi^+\pi^-)} = 2.41 \pm 0.40 \pm 0.12. \quad (3)$$

The comparison of the $\Upsilon(mS) \rightarrow \Upsilon(nS)\eta$ transitions, which are spin-flipping, and the corresponding $\pi^+\pi^-$ ones, that do not require the b -quark spin to flip, is particularly interesting because we naively expect a suppression of the transitions with spin-flipping terms. This is observed for the two vector bottomonium states that are below open b -flavored threshold [3]:

$$\begin{aligned} R_\eta[\Upsilon(2S)] &= (1.63 \pm 0.23) \times 10^{-3}, \\ R_\eta[\Upsilon(3S)] &< 2.29 \times 10^{-3}, \end{aligned} \quad (4)$$

but also in the charmonium sector with $R_\eta[\psi(2S)] = (9.75 \pm 0.17) \times 10^{-2}$ [3]. Note that even for the state which is just close above the c -flavored threshold, and thus it should present a similar role in the charmonium sector than the $\Upsilon(4S)$ in the bottomonium one, the PDG reports a value of $R_\eta[\psi(3770)] = 0.47 \pm 0.22$.

Further insight into the anomalously large $\Upsilon(4S) \rightarrow \Upsilon(1S)\eta$ decay rate can be gained by searching for the transition $\Upsilon(4S) \rightarrow h_b(1P)\eta$ because it is, in principle, dominated by similar spin-flipping contributions. The Belle Collaboration has very recently measured for the first time the branching fraction $\mathcal{B}(\Upsilon(4S) \rightarrow h_b(1P)\eta) = (2.18 \pm 0.11 \pm 0.18) \times 10^{-3}$ [10]. This branching fraction provides a partial decay width of (44.69 ± 6.95) keV when combined with the total decay rate reported by PDG [3]. This value is again unexpectedly large.

The anomalous hadronic decay widths can be due to several mechanisms: Contribution of hadron loops [11–13]; four-quark components in the quarkonium wave

^{*} segonza@usal.es

[†] entem@usal.es

[‡] fdz@usal.es

functions [14]; internal loop radiation [15, 16]; or, as we have pointed out in Ref. [17] and we will see herein, the existence of hybrid mesons with a mass near the one of the decaying resonance¹.

The standard theoretical approach to study hadronic transitions is QCD Multipole Expansion (QCDME) [19–24]. Tung-Mow Yan was the first one to present a gauge-invariant formulation within this framework [25]. Many details about QCDME in the context of the Kuang-Yan model can be found, for instance, in Refs. [26, 27]. The interested reader is also referred to the recent review [28] of Yu-Ping Kuang.

This approach describes the hadronic transition as a two-step process in which the heavy quark system initially emits, at least, two gluons that subsequently hadronize into light hadrons. After the emission of the first gluon and before the emission of the second one, there exists a propagating intermediate state where the $Q\bar{Q}$ pair together with the gluon forms a hybrid state.

Other possibility is to work in a local approximation [24] which does not require the description of hybrid states but it is strictly valid only in the limit of infinite heavy quark mass.

The width of a hadronic transition in QCDME depends critically on the position in the spectrum of the hybrid states, therefore it is important to describe consistently the heavy quarkonia and the hybrids using as few parameters as possible. A description of hybrid mesons is difficult from first principles of QCD [29, 30] and one is generally forced to use models: the flux-tube model [31, 32], constituent gluons [33], Coulomb gauge QCD [34], quark confining string model (QCS) [35–38] or QCD string model [39].

The hadronization vertex is independent of the properties of heavy quarkonium and hybrid states. Usually, this kind of vertices are calculated using low energy theorems [40]. This procedure limits the predictive power of the approach since for each new configuration of initial and final bound states one needs new adjustable parameters. Moreover, for the interesting case of the hadronic transitions involving the η meson one must discard certain operators involving the gluon fields. This last point is relevant for the discussion of this work.

One important feature of the QCDME approach is that the hadronic transitions are classified in a series of chromoelectric and chromomagnetic multipoles. The decay rate of the $\Upsilon(4S) \rightarrow \Upsilon(1S)\eta$ process has two leading multipole gluon emission terms: M1-M1 and E1-M2, whereas the leading order term in the $\Upsilon(4S) \rightarrow \Upsilon(1S)\pi\pi$ transition is an E1-E1 contribution. The M1-M1 term has been usually neglected. However, the hybrid mesons involved in the calculation of the M1-M1 amplitude are different than those involved in the E1-M2/E1-E1 contributions. Therefore, we consider worthy

to estimate in the $\Upsilon(4S) \rightarrow \Upsilon(1S)\eta$ process the M1-M1 term and thus the effect produced in the amplitude by the hybrid meson spectrum before resorting to more sophisticated or exotic mechanisms.

To do this, we will use the QCDME within the same theoretical formalism presented in Ref. [17]. This formalism has explained successfully some puzzles of the two-pion hadronic transitions in the charmonium sector. The branching ratios $R_\eta[\Upsilon(nS)]$ with $n = 2, 3, 4$ will be presented herein². An important feature is that our model for hybrid mesons [17] is a natural, parameter-free extension of a constituent quark model (CQM) [41] (for reviews on the CQM, see Refs. [42, 43]) that describes quite well hadron phenomenology and hadronic reactions [44–46]. Furthermore, the CQM has been recently applied to mesons containing heavy quarks with a remarkable success, describing a wide range of physical observables which concern spectrum [47–49], strong reactions [50–52] and weak decays [53–55].

This manuscript is arranged as follows. In Sec. 2 we introduce the constituent quark model pointing out only those features which are relevant for this work. Section 3 is dedicated to explain the parameter-free extension of our quark model to describe hybrid mesons. Section 4 shows the QCDME formulation of the hadronic transitions highlighting its most relevant features. Our results are provided in Sec. 5. We finish giving some conclusions in Sec. 6.

II. CONSTITUENT QUARK MODEL

The description of the meson spectra is based on the constituent quark model (CQM) proposed by Vijande *et al.* in Ref. [41]. One must solve the Schrödinger equation with a quark-antiquark potential whose main pieces are: i) the Goldstone-boson exchanges between dressed constituent quarks which is a consequence of the dynamical chiral symmetry breaking of QCD, ii) the perturbative one-gluon fluctuations around the instanton vacuum, and iii) a phenomenological confining potential which reflects the empirical fact that quarks and gluons have never been seen as isolated particles. Note that in the heavy quark sector chiral symmetry is explicitly broken and thus Goldstone-boson exchanges do not appear.

Further details about the CQM and the fine-tuned model parameters can be found in Refs. [41, 47, 56]. Here we want to explain in more detail our confinement potential because its screened linear shape is a particular feature of the model. It is well known that multigluon exchanges produce an attractive linearly rising potential proportional to the distance between infinite heavy quarks. However, sea quarks are also important

¹ A similar observation has been also done in Ref. [18].

² A discussion about the goodness of the approach applied to the calculation of the hadronic decays treated herein can be found in Appendix A.

State	Mass (CQM) (MeV)	Mass (Cornell) (MeV)	Mass (Exp.) (MeV)
$\Upsilon(1S)$	9502	9460	9460.30 ± 0.26
$\Upsilon(2S)$	10015	10050	10023.26 ± 0.31
$\Upsilon(3S)$	10349	10400	10355.2 ± 0.5
$\Upsilon(4S)$	10607	10670	10579.4 ± 1.2

Table I. Masses, in MeV, of the S -wave vector bottomonium states up to $n = 4$ predicted by our CQM and by the Cornell model [58, 59]. Experimental masses are taken from PDG [3]. The mass of the $\Upsilon(1S)$ has been fitted in the Cornell potential.

ingredients of the strong interaction dynamics that contribute to the screening of the rising potential at low momenta and eventually to the breaking of the quark-antiquark binding string [57]. Our model try to mimic this behavior using the following expression

$$V_{\text{CON}}(\vec{r}) = [-a_c(1 - e^{-\mu_c r}) + \Delta](\vec{\lambda}_q^c \cdot \vec{\lambda}_{\bar{q}}^c), \quad (5)$$

where a_c and μ_c are parameters, r is the interquark distance and $\vec{\lambda}_{q(\bar{q})}^c$ are $SU(3)$ color matrices. At short distances this potential presents a linear behavior with an effective confinement strength $\sigma = -a_c \mu_c (\vec{\lambda}_q^c \cdot \vec{\lambda}_{\bar{q}}^c)$, while it becomes constant at large distances showing a threshold defined by $V_{\text{thr}} = [-a_c + \Delta](\vec{\lambda}_q^c \cdot \vec{\lambda}_{\bar{q}}^c)$. No $q\bar{q}$ bound states can be found for energies higher than this threshold.

The screened linear potential is a key feature to reproduce the degeneracy pattern observed for the higher excited states of light mesons [56]. As we assume that confining interaction is flavor independent, this affects also to the different quark sectors and, in particular, the bottomonium spectrum. Table I shows the S -wave vector bottomonium states up to $n = 4$ predicted by our quark model. We compare masses with the standard Cornell model [58, 59] and the experimental data reported by PDG [3]. Both models reproduce quite well the experimental data. In the Cornell model the ground state is fitted to the experimental figure while in our case the model parameters are fitted to all meson sectors. One can see that our quark model is able to reproduce in better agreement the excited states which is a particular feature of the screening of the linear confinement potential.

III. A MODEL FOR HYBRIDS

From the generic properties of QCD, we might expect to have states in which the gluonic field itself is excited and carries J^{PC} quantum numbers. A bound-state is called glueball when any valence quark content is absent, the addition of a constituent quark-antiquark pair to an excited gluonic field gives rise to what is called an hybrid meson. The gluonic quantum numbers couple to those of the $q\bar{q}$ pair. This coupling may give rise to so-called

exotic J^{PC} mesons, but also can produce hybrid mesons with natural quantum numbers. We are interested on describing the last ones because they are involved in the calculation of hadronic transitions within the QCME approach.

Ab-initio QCD calculations of the hybrid (even conventional) bottomonium states are particularly difficult because the large mass of the b -quark. Therefore, the only way up to now to describe hybrid mesons in the bottomonium sector is through models. An extension of the quark model described above to include hybrid states has been presented in Ref. [17]. This extension is inspired on the Buchmuller-Tye quark-confining string (QCS) model [35–38] which assumes that the meson is composed of a quark and antiquark linked by an appropriate color electric flux line: the string. Gluon excitation effects are described by the vibration of the string. These vibrational modes provide new states beyond the naive meson picture and are interpreted as hybrid mesons.

The coupled equations that describe the dynamics of the string, quark and antiquark sectors are highly nonlinear so that there is no hope of solving them completely. Then, to introduce the vibrational modes, we use the following approximation scheme. First, we solve the string Hamiltonian via the Bohr-Oppenheimer method to obtain the vibrational energies as a function of the interquark distance [36]

$$V_n(r) = \sigma(r)r \left\{ 1 + \frac{2n\pi}{\sigma(r)[(r-2d)^2 + 4d^2]} \right\}^{1/2}. \quad (6)$$

Note that $n = 0$ gives $V_0(r) = \sigma(r)r$ where $\sigma(r) = (16/3)a_c [(1 - e^{-\mu_c r})/r]$ attending to Eq. (5). The parameter d is the correction due to the finite heavy quark mass

$$d(m_Q, r, \sigma, n) = \frac{\sigma r^2 \alpha_n}{4(2m_Q + \sigma r \alpha_n)}, \quad (7)$$

where α_n is related with the shape of the vibrating string and can take the values $1 \leq \alpha_n \leq \sqrt{2}$.

Second, the vibrational potential is inserted into the meson equation as an effective potential

$$V_{\text{hyb}}(r) = V_{\text{OGE}}(r) + V_{\text{CON}}(r) + [V_n(r) - \sigma(r)r], \quad (8)$$

where $V_{\text{OGE}}(r) + V_{\text{CON}}(r)$ is the naive quark-antiquark potential in the heavy quark sector with $V_{\text{OGE}}(r) = -4\alpha_s/3r$ and $V_{\text{CON}}(r)$ given in Eq. (5). $V_n(r)$ is the vibrational potential calculated above. We must subtract the term $\sigma(r)r$ because it appears twice, one in $V_{\text{CON}}(r)$ and the other one in $V_n(r)$.

We have arrived to a description of the hybrid mesons in the heavy quark sector that does not include new parameters besides those of the original quark model³.

³ The variation of the parameter α_n within its range $[1, \sqrt{2}]$ modifies around 30 MeV the mass of a hybrid state in the bottomonium sector, we have chosen the mean value $\alpha_n = \sqrt{1.5}$.

K / L	0	1
1	10571	10785
2	10857	10999
3	11063	11175
4	11232	11325
5	11374	11452
6	11496	11562
7	11600	11657
8	11690	11738
9	11766	11807
10	11831	11866
11	11885	11913
12	11927	-
$V_{\text{thr}} = 11943$		

Table II. Masses, in MeV, of those hybrid states in the bottomonium sector that participate in the hadronic transitions calculated in this paper. K and L are the hybrid meson quantum numbers.

In that sense, our calculation of the hybrid states is parameter-free. Another important feature of our hybrid model is that, just like the naive quark model, the hybrid potential has a threshold from which no more bound states can be found and so we have a finite number of hybrid states in the spectrum.

Table II shows our theoretical prediction for those hybrid states in the bottomonium sector that will participate in the hadronic transitions in which we are interested. They are classified by the angular momentum L and radial excitation K . It is important to realize here that we predict a hybrid meson with quantum numbers $|KL\rangle = |10\rangle$ which is very close in mass, 10571 MeV, to the $\Upsilon(4S)$ state, 10607 MeV. As we will see later, this feature have important consequences in the calculation of the $\Upsilon(4S)$ hadronic decay rates.

IV. HADRONIC DECAY RATES

The Hamiltonian for a heavy $Q\bar{Q}$ system in QCDME is given by [25]:

$$H_{\text{QCD}}^{\text{eff}} = H_{\text{QCD}}^{(0)} + H_{\text{QCD}}^{(1)} + H_{\text{QCD}}^{(2)}, \quad (9)$$

where $H_{\text{QCD}}^{(0)}$ represents the sum of the kinetic and potential energies of the heavy quarks, $H_{\text{QCD}}^{(1)}$ is related with the color charge of the $Q\bar{Q}$ system (which is zero for color singlets), and $H_{\text{QCD}}^{(2)}$ couples color singlets to octet $Q\bar{Q}$ states. Therefore, the hadronic transitions between eigenstates $|\Phi_I\rangle$ and $|\Phi_F\rangle$ of $H_{\text{QCD}}^{(0)}$ are at least second

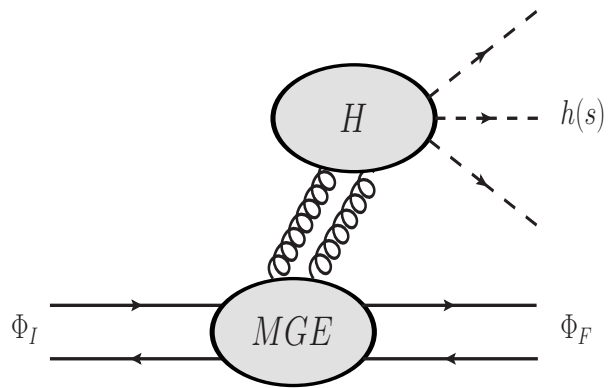


Figure 1. A hadronic transition as a two-step process: (1) emission of gluons from heavy quarks (MGE), and (2) the conversion of gluons into light hadrons (H).

order in $H_{\text{QCD}}^{(2)}$ and the leading term is given by

$$\begin{aligned} \langle \Phi_F h | H_{\text{QCD}}^{(2)} \frac{1}{E_I - H_{\text{QCD}}^{(0)} + i\partial_0 - H_{\text{QCD}}^{(1)}} H_{\text{QCD}}^{(2)} | \Phi_I \rangle &= \\ = \sum_{KL} \langle \Phi_F h | H_{\text{QCD}}^{(2)} | KL \rangle \frac{1}{E_I - E_{KL}} \langle KL | H_{\text{QCD}}^{(2)} | \Phi_I \rangle, \end{aligned} \quad (10)$$

where $|KL\rangle$ with associated energies E_{KL} are intermediate states after the emission of the first gluon and before the emission of the second one. They are the hybrid mesons described in the former Section.

A connection is made to the physical process in Eq. (1) by assuming that the hadronic transition amplitude always splits into two factors (see Fig. 1). The first one concerns the multipole gluon emission (MGE) from the heavy quarks and the second one is an hadronization (H) process describing the conversion of the emitted gluons into light hadron(s).

The MGE vertex involves the wave functions and energies of the initial and final quarkonium states as well as those of the intermediate hybrid mesons. All these quantities are calculated within our model and enter in the hadronic transition rate with integrals of the type⁴:

$$\begin{aligned} f_{IF}^{LP_I P_F} &= \sum_K \frac{1}{M_I - M_{KL}} \left[\int dr r^{2+P_F} R_F(r) R_{KL}(r) \right] \times \\ &\times \left[\int dr' r'^{2+P_I} R_{KL}(r') R_I(r') \right], \end{aligned} \quad (11)$$

⁴ A detailed description of the computation of the decay rates in the single-channel approach of QCDME for the hadronic transitions can be found in Ref. [26]. See also Ref. [28] for an updated review and Ref. [17] for a calculation of two-pion spin-flip hadronic transitions within our model.

where $R_I(r)$ and $R_F(r)$ are, respectively, the radial wave functions of the initial and final states. $R_{KL}(r)$ is the radial wave function of the intermediate vibrational states $|KL\rangle$. The mass of the decaying meson is M_I , whereas the ones corresponding to the hybrid states are M_{KL} .

The H vertex is at the scale of the light hadron(s) and is independent of the properties of the heavy quarkonia and hybrid states. There are two ways of calculating the matrix elements associated with the H factor: (H1) using PCAC and soft pion techniques [25, 40] or (H2) approximating the hadronic transition rates by 2-gluon emission rates [26], for instance, $\Gamma(\Phi_I \rightarrow \Phi_F \eta) \simeq \Gamma(\Phi_I \rightarrow \Phi_F (gg)_{0^-})$ where the two gluons are projected into $J^P = 0^-$ to simulate the η meson.

Certainly, the H2-approach does not take in very detail the conversion of gluonic field(s) into a single η meson. This can be viewed as a crude approximation and one should expect large uncertainties in its predictions. However, it is the only formalism that allows us to treat consistently the M1-M1 amplitude. One could estimate the uncertainties introduced by the H2-approach using the η fragmentation function for the gluons at the scale of interest. This universal nonperturbative object has been calculated, *e.g.*, in Ref. [60] at NLO accuracy and at the scale $\mu = 1$ GeV. The range of values significant for the processes studied here is between 0.25 and 0.50. Therefore, the results predicted by the H2-approach could have a systematic uncertainty of about 50% but not orders of magnitude that can change drastically our conclusions.

The H1 and H2 approaches involve unknown coefficients. However, the difference between the two is that the H1-approach needs, at least, one coefficient for each multipole matrix element (we will denote these coefficients by C_i 's), whereas in the H2-approach all these matrix elements are written in function of only two parameters (g_E and g_M).

We have mentioned in the Introduction that the leading multipoles of an η transition between spin-triplet S -wave states are M1-M1 and E1-M2. Therefore, the matrix element is given schematically by

$$\mathcal{M}(^3S_1 \rightarrow ^3S_1 + \eta) = \mathcal{M}_{M1M1} + \mathcal{M}_{E1M2}. \quad (12)$$

The most extended version of the QCDME formalism, the H1-approach, only considers the E1-M2 multipole gluon emission because it is difficult to find a relation to fix the M1-M1 corresponding parameter, whereas the H2-approach considers both of them. There is no reason to neglect the M1-M1 contribution and this will be a key feature in order to explain the large value of the $\Upsilon(4S) \rightarrow \Upsilon(1S)\eta$ decay rate.

For completeness and because it is important for the discussion in the next Section, we show here the expressions in both approaches for the $^3S_1 \rightarrow ^3S_1 + \pi\pi$

transition:

$$\Gamma_{\pi\pi}^{H1} = G C_1^2 |f_{IF}^{111}|^2, \quad (13)$$

$$\Gamma_{\pi\pi}^{H2} = \left(\frac{g_E^2}{2}\right)^2 \frac{(M_I - M_F)^7}{1890\pi^3} |f_{IF}^{111}|^2, \quad (14)$$

and for the $^3S_1 \rightarrow ^3S_1 + \eta$ transition:

$$\Gamma_{\eta}^{H1} = \frac{8\pi^2}{27} \frac{M_F C_3^2}{M_I m_Q^2} |\vec{q}|^3 |f_{IF}^{111}|^2, \quad (15)$$

$$\Gamma_{\eta}^{H2} = \left(\frac{g_M^2}{3m_Q^2}\right)^2 \frac{1}{12\pi^3} \frac{(M_I - M_F)^7}{140} |f_{IF}^{000}|^2 + \left(\frac{g_E g_M}{3m_Q}\right)^2 \frac{1}{12\pi^3} \frac{(M_I - M_F)^9}{6804} |f_{IF}^{111}|^2, \quad (16)$$

where the factor G is a phase-space integral defined in Eq. (2.4) of Ref. [26], \vec{q} is the momentum of η and $f_{IF}^{LP_I P_F}$ has been defined in Eq. (11).

V. RESULTS

The transitions $\Upsilon(2S) \rightarrow \Upsilon(1S)\pi^+\pi^-$ and $\Upsilon(2S) \rightarrow \Upsilon(1S)\eta$ help us to fix our unknown coefficients. The experimental data [3]

$$\Gamma(\Upsilon(2S) \rightarrow \Upsilon(1S)\pi^+\pi^-) = 5.71 \pm 0.48 \text{ keV}, \quad (17)$$

fixes the constant C_1 in the H1-approach. Once we get C_1 the coefficient g_E is determined through Eqs. (13) and (14). Our values of these two constants are⁵:

$$\begin{aligned} C_1 &= 7.69 \times 10^{-3}, \\ g_E &= 2.17, \end{aligned} \quad (18)$$

which compare well, for instance, with the ones used in the Kuang-Yan model [26].

Now, the constants C_3 and g_M are fixed to the experimental figure of the $\Upsilon(2S) \rightarrow \Upsilon(1S)\eta$ decay rate [3]

$$\Gamma(\Upsilon(2S) \rightarrow \Upsilon(1S)\eta) = (9.27 \pm 1.49) \times 10^{-3} \text{ keV}, \quad (19)$$

and we obtain:

$$\begin{aligned} C_3 &= 2.96 \times 10^{+6} \\ g_M &= 5.70 \end{aligned} \quad (20)$$

which are also compatible with the values reported in Ref. [26] using the Kuang-Yan model.

⁵ Note that the value reported here for C_1 differs to the one used in our previous work [17]: 9.69×10^{-3} , we decided to fit here the bottomonium case instead of the charmonium one in order to eliminate sources of uncertainty. One can realize that the difference is small ($\sim 10\%$) and it is not going to change our conclusions.

Process	H1-approach	H2-approach	Experiment [3]
$\Upsilon(2S) \rightarrow \Upsilon(1S)\pi^+\pi^-$ (keV)	5.71	5.71	5.71 ± 0.48
$\Upsilon(2S) \rightarrow \Upsilon(1S)\eta$ (keV)	9.27×10^{-3}	9.27×10^{-3}	$(9.27 \pm 1.49) \times 10^{-3}$
$R_\eta[\Upsilon(2S)]$	1.62×10^{-3}	1.62×10^{-3}	$(1.64 \pm 0.25) \times 10^{-3}$
$\Upsilon(3S) \rightarrow \Upsilon(1S)\pi^+\pi^-$ (keV)	1.18	0.80	0.89 ± 0.08
$\Upsilon(3S) \rightarrow \Upsilon(1S)\eta$ (keV)	7.59×10^{-3}	20.58×10^{-3}	$< 2.03 \times 10^{-3}$
$R_\eta[\Upsilon(3S)]$	6.43×10^{-3}	25.7×10^{-3}	$< 2.29 \times 10^{-3}$
$\Upsilon(4S) \rightarrow \Upsilon(1S)\pi^+\pi^-$ (keV)	4.01	2.54	1.66 ± 0.24
$\Upsilon(4S) \rightarrow \Upsilon(1S)\eta$ (keV)	12.60×10^{-3}	6.05	4.02 ± 0.76
$R_\eta[\Upsilon(4S)]$	3.14×10^{-3}	2.38	2.42 ± 0.39

Table III. The decay widths, in keV, of the $\Upsilon(3S)$ and $\Upsilon(4S)$ hadronic transitions into $\Upsilon(1S)\pi^+\pi^-$ and $\Upsilon(1S)\eta$ channels. The ratio $R_\eta[\Upsilon(nS)] = \Gamma(\Upsilon(nS) \rightarrow \Upsilon(1S)\eta)/\Gamma(\Upsilon(nS) \rightarrow \Upsilon(1S)\pi^+\pi^-)$ is also given. The experimental data is taken from PDG [3].

Table III shows our theoretical results for the hadronic transitions of the $\Upsilon(3S)$ and $\Upsilon(4S)$ into $\Upsilon(1S)\pi^+\pi^-$ and $\Upsilon(1S)\eta$ channels. The ratio $R_\eta[\Upsilon(nS)] = \Gamma(\Upsilon(nS) \rightarrow \Upsilon(1S)\eta)/\Gamma(\Upsilon(nS) \rightarrow \Upsilon(1S)\pi^+\pi^-)$ for $n = 3, 4$ is also given. The most remarkable feature of this table is the result we obtain for the $R_\eta[\Upsilon(4S)]$. While the ratio predicted within the H1-approach is of the order of 10^{-3} , the calculated value using the H2-approach is of the order of unity and agrees nicely with the experimental measurement.

Our result has a natural explanation. The rate of the $\Upsilon(4S)$ hadronic decay into the $\Upsilon(1S)\eta$ final state has two terms. One is a M1-M1 contribution which involves the hybrid states of $L = 0$ through the term f_{IF}^{000} (see Eq. (16)), whereas the other one is a E1-M2 contribution which involves the $L = 1$ hybrid mesons through the term f_{IF}^{111} (see again Eq. (16)). Therefore, different hybrid intermediate states enter in the calculation of the M1-M1 and E1-M2 terms. Our result indicates that the M1-M1 contribution to the hadronic decay rate can be (very) important because the role played by the $L = 0$ hybrid spectrum.

The $L = 0$ hybrid spectrum should be lower in energy than the $L = 1$ spectrum. This is a general feature, but a model-dependent result is given in Table II. The masses predicted by our model for the ground states of hybrid mesons with $L = 0$ and $L = 1$ are 10.6 GeV and 10.8 GeV, respectively. The $\Upsilon(4S)$ is very close in mass to the ground state of hybrid mesons with $L = 0$, and thus the mass denominator $M_I - M_{KL}$ in Eq. (11) leads to a large enhancement of the $\Upsilon(4S) \rightarrow \Upsilon(1S)\eta$ decay rate through the M1-M1 term. The mass splitting between the $\Upsilon(4S)$ and the ground state of hybrid mesons with $L = 1$ is around 0.2 GeV, which is enough to predict $\Gamma(\Upsilon(4S) \rightarrow \Upsilon(1S)\eta) = 12.92 \times 10^{-3}$ keV when we consider only the E1-M2 term in the H2-approach. Note that this number is very close to the one obtained using the H1-approach.

Table III also shows the $\Upsilon(3S) \rightarrow \Upsilon(1S)\pi^+\pi^-$ and $\Upsilon(3S) \rightarrow \Upsilon(1S)\eta$ decay rates using H1- and H2-approaches. The theoretical widths of the $\Upsilon(3S) \rightarrow \Upsilon(1S)\pi^+\pi^-$ process are compatible with the experimental data, being that of the H2-approach in better agree-

ment with experiment. Only an upper limit of the decay rate for the $\Upsilon(3S) \rightarrow \Upsilon(1S)\eta$ process is reported by PDG [3]. Our predicted values are higher than this upper limit by a factor ~ 3 for the H1-approach and a factor ~ 10 for the H2-approach. The factor is larger in the H2-approach because there are two contributions to the decay rate, M1-M1 and E1-M2. Taking into account only the E1-M2 contribution we obtain $\Gamma(\Upsilon(3S) \rightarrow \Upsilon(1S)\eta) = 2.59 \times 10^{-3}$ which is compatible with the experimental upper limit but still slightly higher. We encourage experimentalists to determine this decay rate with better precision in order to clarify the situation.

A couple of comments are necessary here related with the existence in the literature of alternative explanations to the anomalously large $\Upsilon(4S) \rightarrow \Upsilon(1S)\eta$ decay rate. The enhancement of the branching ratio $R_\eta[\Upsilon(4S)]$ could be attributed to neglect the effect of heavy-meson loops (see the related discussion for the charmonium sector in Refs. [1, 13]). A nonrelativistic effective field theory (NREFT) was introduced in Ref. [12] with the goal of determining the effect of heavy-meson loops on the hadronic transitions between heavy quarkonia with controlled uncertainty. The expansion parameter is the velocity of the heavy mesons in the intermediate state: v_{loop} . The NREFT determines that a typical hadronic transition via heavy-meson loop scales as

$$v_{\text{loop}}^3/(v_{\text{loop}}^2)^2 \times \text{vertex factor}, \quad (21)$$

and, in the case of $R_\eta[\Upsilon(4S)]$, the *vertex factor* accounts for the transition between two S -wave bottomonia which takes place through a $B\bar{B}$ loop via a P -wave vertex. Therefore, the vertex factor is proportional to v_{loop}^2 and the heavy-meson loop contribution scales as order v_{loop} with

$$v_{\text{loop}} \sim \frac{\sqrt{m[\Upsilon(4S)] - 2m[B]}}{m[B]} = 6.26 \times 10^{-2}. \quad (22)$$

Then, heavy-meson loops cannot explain the order of magnitude measured in the branching ratio $R_\eta[\Upsilon(4S)]$.

An alternative explanation for the large decay width of the $\Upsilon(4S) \rightarrow \Upsilon(1S)\eta$ transition has been reported in Ref. [16]. Based on the Field Correlator Method

(FCM) [15], the authors of [16] assume that the η transition between two heavy quarkonia proceeds via intermediate states of BB , BB^* , etc. with the η meson emitted simultaneously at vertices. The dynamics of FCM is different than that of the QCDME and thus it can produce a different outcome for the decay widths. The results within FCM approach can be found in Table 3 of Ref. [16]. The order of magnitude is reproduced for the $\Gamma(\Upsilon(4S) \rightarrow \Upsilon(1S)\eta)$ but a very large value, in strong disagreement with experiment, is also obtained for the decay rate of the $\Upsilon(3S) \rightarrow \Upsilon(1S)\eta$ transition. In order to alleviate this discrepancy, the authors modify their model parameters by (10 – 15)%. Surprisingly, this keeps unmodified all partial decay widths except the $\Gamma(\Upsilon(3S) \rightarrow \Upsilon(1S)\eta)$ that is reduced by 3 orders of magnitude due to cancellations (see again Table 3 of Ref. [16]).

A way to test our picture is computing other hadronic transitions of the $\Upsilon(4S)$ meson in which the $L = 0$ hybrids are involved. One example is the $\Upsilon(4S) \rightarrow h_b(1P)\eta$ transition that has recently been observed by the Belle Collaboration [10] and whose measured branching fraction appears to be anomalously large. The expression for the decay rate of the $\Upsilon(mS) \rightarrow h_b(nP)\eta$ hadronic transitions can be extracted from Eq. (56) of Ref. [28] and reads as

$$\begin{aligned} \Gamma(\Upsilon(mS) \rightarrow h_b(nP)\eta) &= \\ &= \frac{\pi}{1144m_Q^2} \frac{g_M^2}{g_E^2} \frac{M_F|\vec{q}|}{M_I} \left(\frac{4\pi}{\sqrt{6}} f_\pi m_\eta^2 \right)^2 |f_{IF}^{001} + f_{IF}^{110}|^2. \end{aligned} \quad (23)$$

As one can see in Eq. (23), both $L = 0$ and $L = 1$ hybrid states are involved in this kind of transitions through the factors f_{IF}^{001} and f_{IF}^{110} , respectively. We predict

$$\Gamma(\Upsilon(4S) \rightarrow h_b(1P)\eta) = 37.89 \text{ keV}, \quad (24)$$

which is in good agreement with the experimental figure, $(44.69 \pm 6.95) \text{ keV}$. The enhancement of this decay width has the same physical origin than the one found in the decay rate of the $\Upsilon(4S) \rightarrow \Upsilon(1S)\eta$ process: we are predicting a hybrid bottomonium meson which is very close in mass to the $\Upsilon(4S)$. The location of the hybrid mesons in the spectrum is a model-dependent result but our prediction seems to explain two uncorrelated processes, $\Upsilon(4S) \rightarrow \Upsilon(1S)\eta$ and $\Upsilon(4S) \rightarrow h_b(1P)\eta$, even a third one considering our results in Ref. [17]. It is worth to remark again that the construction of our hybrid model does not add any new parameter of a quark model which explains a very large number of hadron phenomenology.

VI. CONCLUSIONS

Recent experiments on the $\Upsilon(4S) \rightarrow \Upsilon(1S)\eta$ and $\Upsilon(4S) \rightarrow h_b(1P)\eta$ transitions have pointed out their

anomalously large decay rates. This seems to contradict the naive expectation that hadronic transitions with spin-flipping terms should be suppressed with respect to those that do not have these terms.

We have studied these transitions within the theoretical framework of a constituent quark model that has been applied successfully to a wide range of hadron observables. In particular, this model has been used in the last few years to study spectra, strong reactions and weak decays in the heavy quark sectors. Therefore, we consider that the quark model parameters are very well constrained for the study of hadronic transitions between heavy quarkonia.

The calculation of the hadronic decay rates has been performed using the QCDME approach. This formalism requires the computation of a hybrid meson spectrum. We have calculated the hybrid states using a natural, parameter-free extension of our quark model based on the Quark Confining String scheme.

The rate of the $\Upsilon(4S) \rightarrow \Upsilon(1S)\eta$ hadronic decay has two leading multipole gluon emission terms: M1-M1 and E1-M2. The M1-M1 term has been usually neglected. We have shown that the hybrid mesons involved in the calculation of the M1-M1 and E1-M2 contributions are different. The M1-M1 contribution involves the hybrid states of $L = 0$, whereas the E1-M2 contribution involves the $L = 1$ hybrid mesons. The $\Upsilon(4S)$ is very close in mass to our predicted ground state of hybrid mesons with $L = 0$, and this leads to a large enhancement of the $\Upsilon(4S) \rightarrow \Upsilon(1S)\eta$ decay rate through the M1-M1 term.

A way to test our prediction against others is looking for hadronic transitions that involve the $L = 0$ hybrids and see if similar enhancements have been observed experimentally. An example is the anomalously large decay rate of the $\Upsilon(4S) \rightarrow h_b(1P)\eta$ process measured recently by the Belle Collaboration. We have shown here that this enhancement has the same physical origin than the one found in the decay $\Upsilon(4S) \rightarrow \Upsilon(1S)\eta$. We must admit that the location of the hybrid mesons in the spectrum is a model-dependent result but our prediction seems to explain the two processes above and even a third one considering our results in Ref. [17].

ACKNOWLEDGMENTS

This work has been partially funded by Ministerio de Ciencia y Tecnología under Contract no. FPA2013-47443-C2-2-P, by the European Community-Research Infrastructure Integrating Activity “Study of Strongly Interacting Matter” (HadronPhysics3 Grant no. 283286), by the Spanish Ingenio-Consolider 2010 Program CPAN (CSD2007-00042) and by the Spanish Excellence Network on Hadronic Physics FIS2014-57026-REDT. J. Segovia acknowledges financial support from a postdoctoral IUFFyM contract of the Universidad de Salamanca, Spain.

Appendix A: GOODNESS OF THE QCDME APPROACH

The QCDME approach is based on performing an expansion of the gluon field $A_\mu^a(\vec{x}, t)$ in Taylor series of $(\vec{x} - \vec{X})$ at the center of mass position \vec{X}^6 :

$$\begin{aligned} A_0^a(\vec{x}, t) &= A_0^a(\vec{X}, t) - (\vec{x} - \vec{X}) \cdot \vec{E}^a(\vec{X}, t) + \dots, \\ \vec{A}^a(\vec{x}, t) &= -\frac{1}{2}(\vec{x} - \vec{X}) \times \vec{B}^a(\vec{X}, t) + \dots, \end{aligned} \quad (\text{A1})$$

where \vec{E}^a and \vec{B}^a are color-electric and color-magnetic fields, respectively.

The Hamiltonian formulation is more convenient when one wants to follow a nonrelativistic formalism. The corresponding Hamiltonian derived from the above formulation is given in Eq. (9) where, more explicitly, $H_{\text{QCD}}^{(2)}$ is

$$H_{\text{QCD}}^{(2)} \equiv -\vec{d}_a \cdot \vec{E}^a(\vec{X}, t) - \vec{m}_a \cdot \vec{B}^a(\vec{X}, t) + \dots, \quad (\text{A2})$$

with

$$\begin{aligned} \vec{d}_a &\equiv g_E \int (\vec{x} - \vec{X}) \Psi^\dagger(\vec{x}, t) \frac{\lambda_a}{2} \Psi(\vec{x}, t) d^3x, \\ \vec{m}_a &\equiv \frac{g_M}{2} \int (\vec{x} - \vec{X}) \times \Psi^\dagger(\vec{x}, t) \vec{\gamma} \frac{\lambda_a}{2} \Psi(\vec{x}, t) d^3x, \end{aligned} \quad (\text{A3})$$

the color-electric dipole moment (E1) and the color magnetic dipole moment (M1) of the $Q\bar{Q}$ system, respectively. Higher-order terms (not shown) give rise to higher-order electric (E2, E3, ...) and magnetic moments (M2, ...).

Since $H_{\text{QCD}}^{(2)}$ couples color-singlet to octet quark-antiquark states, the hadronic transitions are at least second order in $H_{\text{QCD}}^{(2)}$ and the leading term is given by Eq. (10). One realizes that the hadronic decay rate should scale as

$$\langle \Phi_F h | H_{\text{QCD}}^{(2)} | KL \rangle \times \langle KL | H_{\text{QCD}}^{(2)} | \Phi_I \rangle. \quad (\text{A4})$$

For instance and without loss of generality, let us write the amplitude of the QCD multipole expansion approach to the spin-nonflip two pion hadronic transitions between heavy quarkonia:

$$\begin{aligned} \mathcal{M}_{E1E1} &= i \frac{g_E^2}{6} \sum_{KL} \frac{\langle \Phi_F | x_k | KL \rangle \langle KL | x_l | \Phi_I \rangle}{E_I - E_{KL}} \times \\ &\times \langle h | E_k^a E_l^a | 0 \rangle, \end{aligned} \quad (\text{A5})$$

where one is assuming factorization of the heavy-quark interaction and the production of light hadrons. From Eq. (A5), the hadronic decay rate is proportional to

$$(k_F a_F) \times (k_I a_I) = [k_F \langle \Phi_F | x_k | KL \rangle] \times [k_I \langle KL | x_l | \Phi_I \rangle], \quad (\text{A6})$$

⁶ $\vec{X} \equiv (\vec{x}_1 + \vec{x}_2)/2$ is the center of mass position of Q and \bar{Q} , and \vec{x} denotes \vec{x}_1 or \vec{x}_2 .

Initial	Final	L	K	k_F (GeV)	$a_F = \langle \Phi_F r KL \rangle$ (fm)	$k_F a_F$	k_I (GeV)	$a_I = \langle KL r \Phi_I \rangle$ (fm)	$k_I a_I$
$\Upsilon(4S)$	$\Upsilon(1S)$	1	1	1.24	0.20	1.27	0.21	0.016	0.017
		1	2	1.43	0.10	0.74	0.43	0.41	0.89
		1	3	1.58	0.059	0.47	0.61	0.84	2.62
		1	4	1.71	0.038	0.33	0.77	0.054	0.21
		1	5	1.82	0.027	0.25	0.91	0.094	0.43
		1	6	1.91	0.020	0.19	1.03	0.10	0.54
		1	7	1.99	0.015	0.15	1.13	0.087	0.50
		1	8	2.06	0.012	0.13	1.22	0.070	0.43
		1	9	2.11	0.0098	0.10	1.30	0.056	0.37
		1	10	2.16	0.0081	0.088	1.36	0.045	0.31
		1	11	2.20	0.0067	0.075	1.42	0.037	0.26
$\Upsilon(3S)$	$\Upsilon(1S)$	1	1	1.24	0.20	1.27	0.44	0.21	0.46
		1	2	1.43	0.10	0.74	0.66	0.67	2.26
		1	3	1.58	0.059	0.47	0.85	0.066	0.29
		1	4	1.71	0.038	0.33	1.02	0.13	0.66
		1	5	1.82	0.027	0.25	1.16	0.10	0.61
		1	6	1.91	0.020	0.19	1.28	0.078	0.51
		1	7	1.99	0.015	0.15	1.38	0.059	0.41
		1	8	2.06	0.012	0.13	1.48	0.045	0.34
		1	9	2.11	0.0098	0.10	1.55	0.035	0.28
		1	10	2.16	0.0081	0.088	1.62	0.028	0.23
		1	11	2.20	0.0067	0.075	1.68	0.023	0.19
$\Upsilon(2S)$	$\Upsilon(1S)$	1	1	1.24	0.20	1.27	0.79	0.44	1.76
		1	2	1.43	0.10	0.74	1.02	0.16	0.84
		1	3	1.58	0.059	0.47	1.22	0.13	0.82
		1	4	1.71	0.038	0.33	1.39	0.089	0.63
		1	5	1.82	0.027	0.25	1.53	0.061	0.47
		1	6	1.91	0.020	0.19	1.66	0.044	0.37
		1	7	1.99	0.015	0.15	1.77	0.032	0.29
		1	8	2.06	0.012	0.13	1.86	0.025	0.23
		1	9	2.11	0.0098	0.10	1.94	0.020	0.19
		1	10	2.16	0.0081	0.088	2.01	0.016	0.16
		1	11	2.20	0.0067	0.075	2.07	0.013	0.14

Table IV. The relative size of the overlap terms that are involved in the hadronic transitions $\Upsilon(nS) \rightarrow \Upsilon(1S)\pi^+\pi^-$ with $n = 2, 3, 4$.

and not, as usually considered, to $(ka)^2$ with a the average size of the heavy quarkonium states involved in the hadronic transition and k the available momentum of the process.

Table IV shows the relative size of the overlap terms that appear in Eq. (A6) and are involved in the $\Upsilon(4S) \rightarrow \Upsilon(1S)\pi^+\pi^-$ transition. We compare them with those obtained for the $\Upsilon(2S)$ and $\Upsilon(3S)$ states in which usually QCDME approach is considered to work well. One can conclude that QCDME approach works at the same level for the $\Upsilon(4S)$ state than for the $\Upsilon(2S)$ and $\Upsilon(3S)$ states.

REFERENCES

- [1] N. Brambilla, S. Eidelman, B. Heltsley, R. Vogt, G. Bodwin, et al., Eur. Phys. J. **C71**, 1534 (2011).
- [2] G. Abrams et al., Phys. Rev. Lett. **34**, 1181 (1975).
- [3] K. Olive et al. (Particle Data Group), Chin. Phys. **C38**, 090001 (2014).
- [4] I. Adachi et al. (Belle), Phys. Rev. Lett. **108**, 032001 (2012).
- [5] B. Aubert et al. (BaBar), Phys. Rev. Lett. **93**, 041801 (2004).
- [6] B. Aubert et al. (BaBar), Phys. Rev. **D77**, 111101 (2008).
- [7] P. del Amo Sanchez et al. (BaBar), Phys. Rev. **D82**, 011101 (2010).
- [8] J. Lees et al. (BaBar), Phys. Rev. **D86**, 051102 (2012).

- [9] B. Aubert et al. (BaBar), Phys. Rev. **D78**, 112002 (2008).
- [10] U. Tamponi et al. (The Belle Collaboration) (2015), arXiv:hep-ex/1506.08914.
- [11] C. Meng and K.-T. Chao, Phys. Rev. **D77**, 074003 (2008).
- [12] F.-K. Guo, C. Hanhart, and U.-G. Meissner, Phys. Rev. Lett. **103**, 082003 (2009).
- [13] F.-K. Guo, C. Hanhart, G. Li, U.-G. Meissner, and Q. Zhao, Phys. Rev. **D82**, 034025 (2010).
- [14] A. Ali, C. Hambrook, and S. Mishima, Phys. Rev. Lett. **106** (2011), 1011.4856.
- [15] A. Di Giacomo, H. G. Dosch, V. I. Shevchenko, and Yu. A. Simonov, Phys. Rept. **372**, 319 (2002).
- [16] Yu. A. Simonov and A. I. Veselov, Phys. Lett. **B673**, 211 (2009).
- [17] J. Segovia, D. R. Entem, and F. Fernandez, Phys. Rev. **D91**, 014002 (2015).
- [18] H.-W. Ke, J. Tang, X.-Q. Hao, and X.-Q. Li, Phys. Rev. **D76**, 074035 (2007).
- [19] K. Gottfried, Phys. Rev. Lett. **40**, 598 (1978).
- [20] G. Bhanot, W. Fischler, and S. Rudaz, Nucl. Phys. **B155**, 208 (1979).
- [21] M. E. Peskin, Nucl. Phys. **B156**, 365 (1979).
- [22] G. Bhanot and M. E. Peskin, Nucl. Phys. **B156**, 391 (1979).
- [23] M. Voloshin, Nucl. Phys. **B154**, 365 (1979).
- [24] M. B. Voloshin and V. I. Zakharov, Phys. Rev. Lett. **45**, 688 (1980).
- [25] T.-M. Yan, Phys. Rev. **D22**, 1652 (1980).
- [26] Y.-P. Kuang and T.-M. Yan, Phys. Rev. **D24**, 2874 (1981).
- [27] Y.-P. Kuang, Y.-P. Yi, and B. Fu, Phys. Rev. **D42**, 2300 (1990).
- [28] Y.-P. Kuang, Front. Phys. China **1**, 19 (2006).
- [29] K. Juge, J. Kuti, and C. Morningstar, Phys. Rev. Lett. **82**, 4400 (1999).
- [30] J. J. Dudek and E. Rrapaj, Phys. Rev. **D78**, 094504 (2008).
- [31] N. Isgur and J. E. Paton, Phys. Rev. **D31**, 2910 (1985).
- [32] T. Barnes, F. Close, and E. Swanson, Phys. Rev. **D52**, 5242 (1995).
- [33] D. Horn and J. Mandula, Phys. Rev. **D17**, 898 (1978).
- [34] P. Guo, A. P. Szczepaniak, G. Galata, A. Vassallo, and E. Santopinto, Phys. Rev. **D78**, 056003 (2008).
- [35] S. Tye, Phys. Rev. **D13**, 3416 (1976).
- [36] R. Giles and S. Tye, Phys. Rev. **D16**, 1079 (1977).
- [37] W. Buchmuller and S. Tye, Phys. Rev. Lett. **44**, 850 (1980).
- [38] W. Buchmuller and S. H. H. Tye, Phys. Rev. **D24**, 132 (1981).
- [39] Y. Kalashnikova and A. Nefediev, Phys. Rev. **D77**, 054025 (2008).
- [40] L. S. Brown and R. N. Cahn, Phys. Rev. Lett. **35**, 1 (1975).
- [41] J. Vijande, F. Fernandez, and A. Valcarce, J. Phys. **G31**, 481 (2005).
- [42] A. Valcarce, H. Garcilazo, F. Fernandez, and P. Gonzalez, Rept. Prog. Phys. **68**, 965 (2005).
- [43] J. Segovia, D. R. Entem, F. Fernandez, and E. Hernandez, Int. J. Mod. Phys. **E22**, 1330026 (2013).
- [44] F. Fernandez, A. Valcarce, P. Gonzalez, and V. Vento, Phys. Lett. **B287**, 35 (1992).
- [45] H. Garcilazo, A. Valcarce, and F. Fernandez, Phys. Rev. **C63**, 035207 (2001), *ibid.* Phys. Rev. C64, 058201 (2001).
- [46] J. Vijande, H. Garcilazo, A. Valcarce, and F. Fernandez, Phys. Rev. **D70**, 054022 (2004).
- [47] J. Segovia, A. Yasser, D. R. Entem, and F. Fernandez, Phys. Rev. **D78**, 114033 (2008).
- [48] J. Segovia, A. Yasser, D. R. Entem, and F. Fernandez, Phys. Rev. **D80**, 054017 (2009).
- [49] J. Segovia, D. R. Entem, and F. Fernandez, Phys. Rev. **D91**, 094020 (2015).
- [50] J. Segovia, D. R. Entem, and F. Fernandez, Phys. Rev. **D83**, 114018 (2011).
- [51] J. Segovia, D. R. Entem, and F. Fernandez, Phys. Lett. **B715**, 322 (2012).
- [52] J. Segovia, D. R. Entem, and F. Fernandez, Nucl. Phys. **A915**, 125 (2013).
- [53] J. Segovia, C. Albertus, D. R. Entem, F. Fernandez, E. Hernandez, et al., Phys. Rev. **D84**, 094029 (2011).
- [54] J. Segovia, C. Albertus, E. Hernandez, F. Fernandez, and D. R. Entem, Phys. Rev. **D86**, 014010 (2012).
- [55] J. Segovia, E. Hernandez, F. Fernandez, and D. R. Entem, Phys. Rev. **D87**, 114009 (2013).
- [56] J. Segovia, D. Entem, and F. Fernandez, Phys. Lett. **B662**, 33 (2008).
- [57] G. S. Bali, H. Neff, T. Duessel, T. Lippert, and K. Schilling (SESAM), Phys. Rev. **D71**, 114513 (2005).
- [58] E. Eichten, K. Gottfried, T. Kinoshita, K. Lane, and T.-M. Yan, Phys. Rev. **D17**, 3090 (1978).
- [59] E. Eichten, K. Gottfried, T. Kinoshita, K. Lane, and T.-M. Yan, Phys. Rev. **D21**, 203 (1980).
- [60] C. A. Aidala, F. Ellinghaus, R. Sassot, J. P. Seele, and M. Stratmann, Phys. Rev. **D83**, 034002 (2011).